Proc. Natl. Acad. Sci. USA
Vol. 91, pp. 1229–1233, February 1994
Biophysics

Time-dependent diffusion of water in a biological model system

(erythrocytes/pulsed-field gradient NMR/cerebral ischemia/membrane permeability/effective medium theory)

LAWRENCE L. LATOUR*, KAREL SVOBODA†‡§, PARTHA P. MITRA¶, AND CHRISTOPHER H. SOTAK*‖

*Department of Biomedical Engineering, Worcester Polytechnic Institute, Worcester, MA 01609; †Committee on Biophysics and ¶Department of Physics, Harvard University, Cambridge, MA 02138; and ‖Department of Radiology, University of Massachusetts Medical School, Worcester, MA 01655

Communicated by Bertrand I. Halperin, November 9, 1993 (received for review March 29, 1993)

ABSTRACT **Packed erythrocytes are ideally suited as a model system for the study of water diffusion in biological tissue, because cell size, membrane permeability, and extracellular volume fraction can be varied independently. We used a pulsed-field-gradient spin echo NMR technique to measure the time-dependent diffusion coefficient $D(t)$ in packed erythrocytes. The long-time diffusion constant, D_{eff}, depends sensitively on the extracellular volume fraction. This may explain the drop in D_{eff} during the early stages of brain ischemia, where just minutes after an ischemic insult the extra-cellular volume in the affected region of the brain is significantly reduced. Using an effective medium formula, we estimate the erythrocyte membrane permeability, in good agreement with measurements on isolated cells. From the short-time behavior of $D(t)$, we determine the surface-to-volume ratio of the cells, $\approx(0.72\ \mu m)^{-1}$.**

Diffusive transport of water in the presence of permeable membranes is of fundamental biological importance (1). The measured diffusion coefficient, $D(t)$, depends on observation time and is a sensitive function of several physical parameters: membrane permeability, κ; the volume fraction of connected extracellular fluid, ϕ; and local water concentrations. The geometrical arrangement of the membranes is important in determining $D(t)$, and ϕ is a parameter that characterizes this arrangement. Samples of erythrocytes (RBCs) are ideally suited for the study of such effects since cell size, κ, and ϕ can all be independently controlled. The pulsed-field-gradient (PFG) NMR technique (2) has been used to determine the membrane permeability of biological membranes in packed RBCs and some types of tissue (3, 4). To derive κ from the effective (long time) diffusion coefficient, D_{eff}, these studies utilized the relation, noted by Crick (5),

$$\frac{1}{D_{eff}} = \frac{1}{D_0} + \frac{1}{\kappa a}, \qquad [1]$$

where D_0 is the bulk diffusion coefficient and a the spacing between a periodic array of parallel barriers of permeability κ. For most biological tissue this formula is deficient in the following ways: (*i*) It does not provide for different diffusion coefficients in different compartments. (*ii*) The one-dimensional array of membranes cannot capture the effect of parallel diffusion pathways on the diffusion coefficient (Fig. 1). As a result, Eq. 1 predicts that $D_{eff} \to 0$ as $\kappa \to 0$, which is not the case for cells surrounded by extracellular water. Quasi one-dimensional models that incorporate extracellular diffusion pathways have been proposed (6, 7). These models are of limited applicability and we will not discuss them further. (*iii*) Eq. 1 does not account for differences of absolute concentrations of water in different compartments. For example, the second term on the righthand side should be replaced by $c/(\kappa a)$ if, in the space between membranes, other molecules such as proteins occupy a fractional concentration $1 - c$. This effect is in addition to the change in the microscopic diffusion coefficient of water produced by the presence of the proteins.

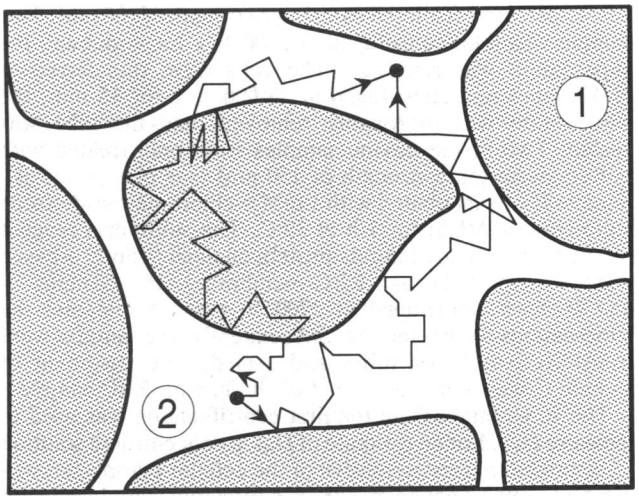

FIG. 1. Cartoon of a sample of packed RBCs. Intracellular (cytoplasmic) fluid [33% (wt/vol) hemoglobin] with water diffusion coefficient, D_{int}, and fractional water concentration c_{int} is shown as stippled areas numbered 1. Extracellular fluid with diffusion coefficient D_{ext} and water concentration c_{ext} is shown as the open area numbered 2. Also shown are two parallel diffusion pathways, one of which is not accounted for in Eq. 1.

PFG NMR is an ideal tool for measuring the time-dependent diffusion coefficient (2). The measurement is nondestructive and does not involve the introduction of chemical or isotopic tracers. The observation time can be varied over several orders of magnitude. The minimum observation time is determined by the minimum length of gradient pulses and the subsequent recovery of the apparatus from eddy current and magnetoacoustic effects and by signal-to-noise considerations. The maximum time is determined by the spin–lattice and spin–spin relaxation times of the fluid. We used PFG NMR to study the effects of ϕ and κ on D_{eff}. Using an effective medium theory (EMT), we calculate κ from measured values of D_{eff}. We also measured the time dependence of the diffusion coefficient at short times. Our data are consistent with recent work on porous media with solid grains (8, 9) and demonstrate that the surface-to-volume

The publication costs of this article were defrayed in part by page charge payment. This article must therefore be hereby marked "*advertisement*" in accordance with 18 U.S.C. §1734 solely to indicate this fact.

Abbreviations: PFG, pulsed-field gradient; EMT, effective medium theory; RBC, erythrocyte; pCMBS, *p*-chloromercuribenzene sulfonate.

‡Present address: Rowland Institute for Science, 100 Edwin Land Boulevard, Cambridge, MA 02142.
§To whom reprint requests should be sent at the present address.

ratio of biological membranes can be estimated using PFG NMR.

MATERIALS AND METHODS

Four types of samples were studied, one consisting of human RBCs and three of bovine RBCs (samples A, B, and C). Blood was stored and handled in air and, therefore, contained diamagnetic oxyhemoglobin. Fresh blood was washed in physiological buffered saline (PBS; 150 mM ionic strength). All buffers were adjusted to pH 7.4 and contained 1 mM NaN_3. RBC volumes decrease with increasing extracellular salt concentrations. To swell the cells, human RBCs were suspended in PBS diluted to an ionic strength of 100 mM. This sample was then centrifuged at 2700 × *g* for 4 min and the supernatant was removed. The cells were transferred to NMR tubes and centrifuged at 23,000 × *g* for 15 min, the supernatant was thoroughly removed, and the tube was sealed. Two of the bovine samples were only treated with buffers at an ionic strength of 150 mM (samples A and B). Sample B was incubated with 1 mM *p*-chloromercuribenzene sulfonate (pCMBS) for 1 h at 30°C. The sulfhydryl reagent pCMBS specifically inhibits protein channel ("pore")-based water transport through RBC membranes (10). Samples A and B were centrifuged at 2700 × *g* for 4 min and the supernatants were removed. Subsequently, the samples were transferred to NMR tubes and sealed. The treatment of sample C was identical to that of the human RBC sample.

The supernatant from the first centrifugation was used to measure D_{ext}. For an estimate of D_{int}, a concentrated solution of hemoglobin, representative of the cellular cytoplasm, was purified: RBCs packed at 2700 × *g* for 4 min were lysed with 10 vol of hypotonic buffer (1 mM ionic strength). The solution was centrifuged at 23,000 × *g* for 15 min to pellet ghosts and the supernatant was concentrated 11-fold in a protein dialysis membrane (ProDiMem PA-30, Bio-Molecular Dynamics, Beaverton, OR). To estimate D_{int} in swollen cells (100 mM ionic strength), we added 30% of buffer to the concentrate (11).

Cell concentrations were measured using a hemacytometer counting chamber at 1:1000 cell dilutions (Fisher Scientific). We assumed a hexagonal close packing to compute cell center spacings from cell concentrations. The sphere equivalent radii were computed from the cell concentrations of cells packed at 23,000 × *g* for 15 min. For these samples, we assumed zero extracellular volume fraction, $\phi = 0$ (human RBCs and sample C). This is consistent with differential interference contrast (DIC) optical microscopy (data not shown). For samples packed at 2700 × *g*, ϕ was not equal to 0 (samples A and B). We took ϕ to be the supernatant volume fraction obtained after the same sample was centrifuged at 23,000 × *g*. We assume that the RBC cell volume does not depend on the centripetal force at these speeds, consistent with DIC microscopy. To determine cell surface areas, we lysed RBCs (5 mM ionic strength on ice) and immediately measured the diameters of spherical ghosts using DIC microscopy (12).

Diffusion measurements were made at 23°C in a GE CSI 2T/45 cm imaging spectrometer operating at 85.56 MHz for protons. The gradient coils were self-shielded with a 32-mm bore and were capable of delivering up to ±280 G/cm. A modified stimulated echo sequence (13, 14) was used to reduce the effect of internal magnetic field gradients. In this sequence, pairs of bipolar gradient pulses interleaved with π pulses are used instead of a single gradient pulse. The π pulses serve to refocus the dephasing due to internal gradients. To obtain $D(t)$, the magnetization, $M(\mathbf{k},t)$, was measured at a fixed t for 10 values of $\mathbf{k}$, where $\mathbf{k} = \gamma \mathbf{G} \delta$, and the slope was obtained from a plot of ln $M(\mathbf{k},t)$ vs. $\mathbf{k}^2$. $D(t)$ was measured at 20 values of t by using even increments in $\sqrt{t}$ and the quantity $\mathbf{k}_{max}^2 t$ was held constant. Diffusion measurements were repeatable with blood up to 10 days old. This demonstrates that the effects of possible changes in blood oxygenation were small.

The interpretation of PFG NMR data in terms of the diffusion propagator is complicated by the effects of finite pulse widths, magnetic field inhomogeneities, and surface relaxation. The first effect is the most significant, but it can be accounted for both at short and long times (9). Nonlinear internal gradients cannot be eliminated by the pulse sequence used. Unrefocused internal inhomogeneities lower the apparent diffusion coefficient. Since observed linewidths were narrow (≈20 Hz), we expect this effect to be small. Surface relaxation affects the diffusion coefficient only by subleading terms, and since measured spin-lattice relaxation times (T_1) in the samples were relatively long (≈1 s), we conclude that effects of surface relaxation on our diffusion measurements are small.

THEORY

Long-Time Diffusion Constant. We define the time-dependent diffusion coefficient as $D(t) = \langle r^2(t) \rangle / (6t)$, where $\langle r^2(t) \rangle$ is the mean square displacement of the diffusing water molecules. At long times, $D(t)$ saturates, $\lim_{t \to \infty} D(t) = D_{eff}$. To generalize Eq. 1, we developed an EMT for D_{eff}. The RBCs are modeled as spheres of radius a with membrane permeability κ. Other parameters of the theory are intra- and extracellular diffusion coefficients, D_{int} and D_{ext}; intra- and extracellular water concentrations (vol/vol), c_{int} and c_{ext}; and the volume fraction of extracellular fluid, ϕ, forming a connected network of diffusion pathways. The EMT formula is (see *Appendix*)

$$\left(\frac{D_{eff} c_{eff} - D_1 c_{int}}{D_{ext} c_{ext} - D_1 c_{int}} \right) \left(\frac{D_{ext} c_{ext}}{D_{eff} c_{eff}} \right)^{1/3} = \phi, \qquad [2]$$

where

$$D_1 c_{int} = \frac{\kappa a D_{int} c_{int}}{\kappa a + D_{int} c_{int}} \qquad [3]$$

and $c_{eff} = \phi c_{ext} + (1 - \phi) c_{int}$. In the limit $\phi = 0$, the formula becomes $1/D_{eff} = (1/D_{int}) + c_{int}/(\kappa a)$. The concentration factor is significant since for RBCs, $c_{int} = 0.71$ (15). For finite ϕ, the EMT accounts for enhanced diffusion due to parallel extracellular pathways (Figs. 1 and 2). The effective diffusion coefficient depends strongly on ϕ (Fig. 2). In the limit $\kappa = 0$, the EMT reduces to $D_{eff} c_{eff} = D_{ext} c_{ext} \phi^{3/2}$, analogous to the well-known empirical rule in porous media termed Archie's law (16). In contrast with diffusion in porous media with solid grains, here the diffusion coefficient scales with an extra factor of ϕ. This is due to the water contained in the impermeable spheres. Changing cell shape should not affect the qualitative conclusions of our analysis (Fig. 2 and *Appendix*).

***D(t)* at Short Times.** The time dependence of the diffusion coefficient has been studied for a periodic array of parallel membranes (17), but in this work an important point has been missed: at short times, the diffusion coefficient decreases from its bulk value with a universal $\sqrt{t}$ behavior depending only on the surface-to-volume ratio (S/V) of the membranes. This behavior, namely,

$$D(t) = D_0 \left(1 - \frac{4}{9\sqrt{\pi}} \times \frac{S\sqrt{D_0 t}}{V} \right) + \mathcal{O}(D_0 t) \qquad [4]$$

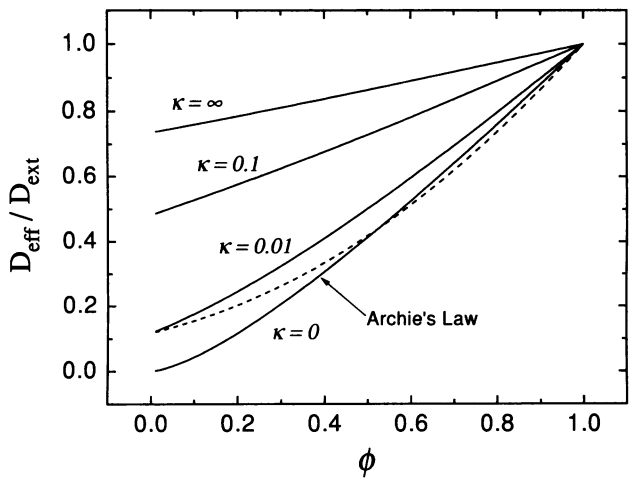

FIG. 2. D_{eff} as a function of extracellular volume fraction given by Eq. 2 (solid lines; $\kappa = 0, 0.01, 0.1, \infty$ cm/s) and Eq. 8 (dashed line; $\kappa = 0.01$ cm/s). Parameter values: $D_{int} = 1.56 \times 10^{-5}$ cm^2/s, $D_{ext} = 2.12 \times 10^{-5}$ cm^2/s, $c_{ext} = 1$, $c_{int} = 0.71$, and $a = 2.1$ μm. The region of biological interest is bounded by the $\kappa = 0$ and $\kappa = 0.01$ lines.

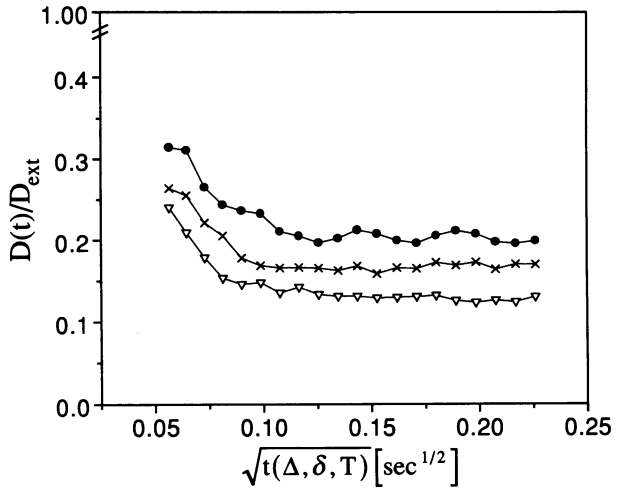

FIG. 3. $D(t)$ of water in packed bovine RBCs in three samples with equal membrane densities. ●, Lightly packed at 2700 × g for 4 min, ionic strength at 150 mM, with ≈19% extracellular fluid; ×, same conditions except that the membrane permeability was reduced by incubation with 1 mM pCMBS; ▽, packed at 23,000 × g for 15 min, ionic strength at 100 mM, with essentially no extracellular fluid. D_{ext} is the bulk extracellular fluid diffusion constant.

has been predicted (8) to occur in porous media with hard walls, but an extension shows that the same short-time behavior holds for permeable membranes. The reason is the following: the relevant dimensionless combination including κ is $\kappa tS/V$, and at short times $\kappa tS/V << (4/9\sqrt{\pi})(S\sqrt{D_0 t}/V)$; the term involving κ is, therefore, of higher order than the $\sqrt{t}$ term. Other subleading terms in Eq. 4 are of order $(S/V)D_0 t\langle R^{-1}\rangle$, where $\langle R^{-1}\rangle$ is the mean curvature of the membranes (9). In the presence of multiple compartments, Eq. 4 generalizes to an arithmetic average over different compartments. Eq. 4 provides a technique for determining S/V in biological membrane systems. We emphasize that Eq. 4 holds for piecewise smooth surfaces of arbitrary geometry.

RESULTS

To study the effects of κ and ϕ on D_{eff}, we chose three bovine RBC samples (A, B, and C) with equal membrane densities (cell-to-cell spacing ≈4.1 ± 0.1 μm, $N = 4$). For RBCs at 150 mM ionic strength packed at 2700 × g for 4 min (sample A), D_{eff} was 0.42 × 10^{-5} cm^2/s, lower than the diffusion coefficient of the extracellular bulk fluid (2.12 × 10^{-5} cm^2/s) (Fig. 3). For sample B, κ was reduced by incubation with pCMBS, which led to a further decrease to $D_{eff} = 0.35 \times 10^{-5}$ cm^2/s. Sample C differed from sample A by a reduced ϕ with κ unchanged. In this sample, D_{eff} was 0.27 × 10^{-5} cm^2/s. D_{eff} in sample C was 60% lower than in sample A, although the membrane permeabilities were the same. The drop in D_{eff} for sample C is due to a reduction of the extracellular pathways. The drop in D_{eff} in sample B is exclusively due to a decrease in κ, the extracellular pathways being left unaltered.

To derive κ from D_{eff} and Eqs. 2 and 3, we measured the diffusion coefficients of the intra- and extracellular bulk fluids (Table 1; $D_{ext} = 2.12 \times 10^{-5}$ cm^2/s). The volume fraction of water in the hemoglobin-rich cytoplasm is 0.71 at 150 mM (15) and 0.78 at 100 mM [assuming a 30% increase in cell volume (11)]. The extracellular fluid in washed RBC samples is protein-free buffer and thus $c_{ext} = 1$. The parameters ϕ and a were estimated from cell counting.

In bovine RBCs, $D(t)$ at 3 ms is only a factor of ≈1.5 larger than D_{eff} (Fig. 3). Human RBCs are larger (cell surface areas: human RBCs, 127.5 ± 9.8 μm^2; bovine RBCs, 73.9 ± 10.4 μm^2). Therefore, the short-time behavior of the diffusion constant was more easily accessible in samples of human RBCs (Fig. 4). The short-time formula, Eq. 4, as applied to PFG NMR experiments, is only valid for δ function sharp pulses. To interpret data from the actual pulse sequence, we corrected for finite pulse width as described (9). We replaced t in Eq. 4 by a function of sequence parameters, $t(\Delta,\delta,T)$, derived from the same expansion that leads to Eq. 4. The horizontal axis in Figs. 3 and 4 is $\sqrt{t(\Delta,\delta,T)}$. The minimum observation time corresponds to $t = 3$ ms. Even the human RBCs were too small to observe the linear in $\sqrt{t(\Delta,\delta,T)}$ behavior of $D(t)$. To test whether the data we do obtain are consistent with the rigorous result (Eq. 4), we used a Padé approximant (18), in this case a ratio of two quadratic polynomials (solid curve, Fig. 4), to interpolate between the short-time (Eq. 4) and the long-time (9) limits. This interpolation formula gives an estimate of the slope of $D(t)$ as a function of $\sqrt{t(\Delta,\delta,T)}$ at short times. The $t = 0$ intercept was fixed to the bulk diffusion coefficient found in the cytoplasm. This procedure is justified because we observe significant time dependence in $D(t)$, and over the observation range, $D(t)$ falls by a factor of ≈3 (Fig. 4 *Inset*). Applying Eq. 4 to the short-time slope of the Padé approximant, we obtain $V/S = 0.72 \pm 0.15$ μm, in agreement with the value obtained from microscopy (0.90 ± 0.1 μm).

Table 1. Measured parameter values and computed permeabilities

Sample	D_{eff}, ×10^{-5} cm^2/s	a, μm	ϕ	c_{int}	D_{int}, ×10^{-5} cm^2/s	κ, ×10^{-3} cm/s
A	0.42	2.1	0.19	0.71	1.56	6.3 ± 1.4
B	0.35	2.1	0.19	0.71	1.56	3.7 ± 1.3
C	0.27	2.3	0.00	0.78	1.64	11.0

Standard errors: D_{eff} and D_{int}, ±0.01 × 10^{-5} cm^2/s; a, ±0.1 μm; ϕ, ±0.02 (except sample C). For κ, computed errors are dominated by errors in ϕ. Since we assumed $\phi = 0$ for sample C, an error estimate could not be given for this sample.

DISCUSSION

Membrane Permeabilities. The calculated membrane permeability for sample A (see Table 1) is in approximate agreement with measurements on isolated RBCs (typically, $\kappa = 5 \times 10^{-3}$ cm/s) (15, 19). Treatment with 1 mM pCMBS results in an ≈50% reduction in the membrane permeability by blocking the protein-channel-based water transport while leaving the lipid-based pathways unchanged (1, 10). The observed 40% reduction of κ after addition of pCMBS (compare samples A and B) is consistent with these facts. For sample C, the calculated permeability is too large. Since κ, as determined by Eqs. 2 and 3, is a sensitive function of ϕ, the discrepancy may be due to an underestimate of ϕ in the experimental preparations (ϕ was estimated to be 0 for sample C).

Other studies employing PFG NMR for examining packed RBC samples have used Eq. 1 to derive κ, which neglects extracellular pathways, and have thus overestimated the membrane permeability [$\kappa = 0.014$ cm/s (3)]. Alternative methods to determine membrane permeability rely on the fact that isolated cells are available. This requirement makes these methods not applicable to measurements in tissue. We have shown that a good estimate of the permeability can be obtained from D_{eff} provided the extracellular pathways are properly accounted for, and our effective medium formula can be used for this purpose. D_{eff} depends sensitively on the extracellular volume fraction (Figs. 2 and 3), a parameter that is likely to be difficult to estimate accurately. An alternative approach to measuring κ could be based on the fact that one of the terms linear in t in the expansion of $D(t)$ (Eq. 4) contains a factor of κ.

***D*eff in Cerebral Ischemia.** One motivation for this work was to develop a model that could be used to help our understanding of diffusion in more complex biological tissue, such as the central nervous system. D_{eff} in the normal brain has been found to be 2–10 times slower than that of free water (20, 21). Early detection of cerebral ischemia is potentially an important clinical application of PFG measurements of diffusion in the brain (22). Within 1 h after the occlusion of the middle cerebral artery in animal models of focal ischemia, D_{eff} (at 40 ms) in the affected region of the brain decreases by up to 50% (23). The mechanism of this drop in D_{eff} is unknown. It is known, however, that cerebral ischemia is accompanied by the massive entry of extracellular ions and water into the intracellular space, leading to a reduction of the extracellular volume fraction (24), from $\phi = 0.20$ to $\phi = 0.11$ (25). This change in ϕ can account for the drop in D_{eff}. By using typical values for the parameters of our EMT ($\kappa = 10^{-3}$ cm/s; $D_{ext} = D_{int} = 3.0 \times 10^{-5}$ cm^2/s; $c_{int} = c_{ext} = 0.8$; $a = 5$ μm), we calculate $D_{eff}(\phi = 0.20) = 3.5 \times 10^{-6}$ cm^2/s and $D_{eff}(\phi = 0.11) = 1.9 \times 10^{-6}$ cm^2/s, a 45% drop in the diffusion constant. Although the EMT formula was derived for spherical cell shapes, it should give qualitatively correct results for more complicated geometries. This is because it captures the following important physical point: since biological membrane permeabilities are small, the dominant contribution to D_{eff} comes from diffusion pathways that go around the cells rather than those that cross cell membranes (Fig. 1). This point is further illustrated by D_{eff} computed for diffusion perpendicular to cylindrical cells (Fig. 2 and *Appendix*). Others have argued that a change in the membrane permeability may explain the observed drop in D_{eff}.** We consider this possibility unlikely, for two reasons: (*i*) For biologically relevant values of the permeability ($\kappa < 10^{-2}$), ϕ is the main determinant of D_{eff} (Fig. 2). (*ii*) As we have shown, the observed change in ϕ could account for the observed change in D_{eff}.

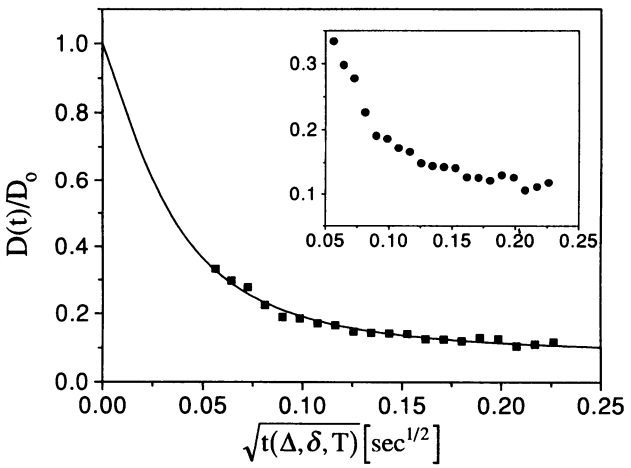

FIG. 4. $D(t)$ of water in packed human RBCs (100 mM NaCl, packed at 23,000 × *g* for 15 min). Solid curve is the Padé approximant fit to the data. From Eq. 4, we estimate $V/S \approx 0.72 \pm 0.15$ μm. D_0 is the cytoplasmic diffusion constant.

Surface to Volume Ratio. We have shown that measuring the short time transient behavior of $D(t)$ is a potential way of determining the surface-to-volume ratio of biological membranes. Although we could not reach short enough times to observe the $\sqrt{t(\Delta,\delta,T)}$ behavior of the diffusion constant directly, our data had substantial time dependence and allowed us to estimate S/V. As far as we know, there is no other noninvasive method for measuring this parameter. The shortest available observation times are set by effects such as eddy currents. We can expect that technical improvements will make it possible to probe shorter times and thus obtain S/V with greater accuracy. Absence of time dependence of the measured diffusion constant has sometimes been interpreted as the absence of restrictions to the diffusion (20). Our study shows that this may simply arise from not probing times short enough to see the effects of restrictions.

APPENDIX

Eq. 2 is analogous to the results of the effective medium theory for conductivity in porous media (26, 27). Consider a spherical cell bounded by a membrane of permeability κ and radius a, containing a volume fraction c_1 of water with diffusion coefficient D_1, immersed in extracellular fluid containing a volume fraction c_2 of water with diffusion coefficient D_2. Let us denote the density of a set of tagged molecules inside and outside the cell by $\rho_1(\mathbf{x})$ and $\rho_2(\mathbf{x})$, respectively. The current of tagged molecules is given by $\mathbf{J} = -D\nabla\rho$. The boundary conditions at the cell surface are $(\mathbf{J}_1 - \mathbf{J}_2)\cdot\hat{\mathbf{n}}_{1\to2} = 0$ and $\mathbf{J}_1\cdot\hat{\mathbf{n}}_{1\to2} = \kappa(\rho_1/c_1 - \rho_2/c_2)$. First, we consider the situation where a single cell is placed in a uniform concentration gradient and perturbs the uniform current $J_0\hat{z}$. The spatial variation of ρ_2 is then given by

$$\rho_2(\mathbf{x}) = \frac{J_0}{D_2}\left[-r\cos(\theta) + \frac{D_{in}c_1 - D_2c_2}{D_{in}c_1 + 2D_2c_2} \times \frac{a^3\cos(\theta)}{r^2}\right], \quad [5]$$

with $(D_{in}c_1)^{-1} = (\kappa a)^{-1} + (D_1c_1)^{-1}$. Next we consider N such cells uniformly distributed in a spherical region of radius R. If the cells are placed sufficiently far apart, then each of them perturbs the density independently in the same manner as described by ref. 26. The total perturbation, at a distance $r >> R$, is then given by N times the perturbation of a single

**Helpern, J. A., Ordidge, R. J. & Knight, R. A., 11th Annual Scientific Meeting of the Society of Magnetic Resonance in Medicine, Berlin, August 8–11, 1992, p. 1201 (abstr.).

sphere located at the center of the region. Equating this to the perturbation caused by a single large sphere of radius R and an effective diffusion constant D_{eff}, we obtain

$$\frac{D_{\text{eff}}c_{\text{eff}} - D_2c_2}{D_{\text{eff}}c_{\text{eff}} + 2D_2c_2} = f\frac{D_{\text{in}}c_1 - D_2c_2}{D_{\text{in}}c_1 + 2D_2c_2}, \quad [6]$$

where f is the volume fraction occupied by the cells, and $c_{\text{eff}} = c_1f + c_2(1 - f)$. This equation holds for a dilute suspension of cells. As the concentration of cells increases, we can use a differential version of Eq. **6**. In this approach, we consider adding cells a few at a time to an initial volume of extracellular fluid to finally reach the desired concentration. At each stage, the cells and extracellular fluid already present are considered to be a homogeneous medium with diffusion constant given by the as yet unknown effective medium formula. Eq. **6** is used to compute the effective diffusion constant after each addition of a small number of cells. This leads to a differential equation governing the effective diffusion constant:

$$\frac{d\log(D_{\text{eff}}c_{\text{eff}})}{d\log\phi} = 3\frac{D_{\text{eff}}c_{\text{eff}} - D_{\text{in}}c_1}{2D_{\text{eff}}c_{\text{eff}} + D_{\text{in}}c_1}, \quad [7]$$

where ϕ is the extracellular fluid fraction. On integrating this differential equation with $D_{\text{eff}}c_{\text{eff}} = D_{\text{ext}}c_{\text{ext}}$ at $\phi = 1$, we obtain Eq. **2**. The power 1/3 is related to the depolarization factor of a sphere. A similar calculation for diffusion perpendicular to permeable cylindrical cells gives

$$\left(\frac{D_{\text{eff}}c_{\text{eff}} - D_1c_{\text{int}}}{D_{\text{ext}}c_{\text{ext}} - D_1c_{\text{int}}}\right)\left(\frac{D_{\text{ext}}c_{\text{ext}}}{D_{\text{eff}}c_{\text{eff}}}\right)^{1/2} = \phi. \quad [8]$$

The ϕ dependence of D_{eff} is qualitatively similar in both cases (see Fig. 2).

We thank H. C. Berg, D. Branton, B. I. Halperin, R. L. Kleinberg, and P. N. Sen for advice. We also acknowledge loans of equipment from H. C. Berg, S. M. Block, and D. Branton. This work was supported in part by Schlumberger–Doll Research, the Rowland Institute of Science, and National Science Foundation Grant DMR-91-15491.

1. Finkelstein, A. (1987) *Water Movement Through Lipid Bilayers, Pores, and Plasma Membranes: Theory and Reality* (Wiley–Interscience, New York).
2. Stejskal, E. O. & Tanner, J. E. (1965) *J. Chem. Phys.* **42,** 288–292.
3. Cooper, R. L., Chan, D. B., Young, A. C., Martin, C. J. & Ancker-Johnson, B. (1974) *Biophys. J.* **14,** 161–177.
4. Tanner, J. E. (1983) *Arch. Biochem. Biophys.* **224,** 416–428.
5. Crick, F. (1970) *Nature (London)* **225,** 420–422.
6. Redwood, W. R., Rall, E. & Perl, W. (1974) *J. Gen. Physiol.* **64,** 706–729.
7. Klosgen, B., Schonert, H. & Deuticke, B. (1988) *Biochim. Biophys. Acta* **939,** 29–39.
8. Mitra, P. P., Sen, P. N., Schwartz, L. M. & Le Doussal, P. (1992) *Phys. Rev. Lett.* **68,** 3555–3558.
9. Latour, L. L., Mitra, P. P., Kleinberg, R. L. & Sotak, C. H. (1993) *J. Magn. Reson.* **101,** 342–346.
10. Macey, R. Y. & Farmer, R. E. L. (1970) *Biochim. Biophys. Acta* **211,** 104–106.
11. Endre, Z. H., Kuchel, P. W. & Chapman, B. E. (1984) *Biochim. Biophys. Acta* **803,** 137–144.
12. Svoboda, K., Schmidt, C. F., Branton, D. & Block, S. M. (1992) *Biophys. J.* **63,** 784–795.
13. Cotts, R. M., Hoch, M. J. R., Sun, T. & Marker, J. T. (1989) *J. Magn. Reson.* **83,** 252–266.
14. Latour, L. L., Li, L. & Sotak, C. H. (1993) *J. Magn. Reson.* **101,** 72–77.
15. Solomon, A. K. (1989) *Methods Enzymol.* **173,** 192–222.
16. Archie, G. E. (1942) *Trans. Am. Inst. Min. Eng.* **146,** 54.
17. Tanner, J. E. (1978) *J. Chem. Phys.* **69,** 1748–1754.
18. Bender, C. M. & Orszag, S. A. (1978) *Advanced Mathematical Methods for Scientists and Engineers* (McGraw–Hill, New York).
19. Farmer, R. E. L. & Macey, R. Y. (1970) *Biochim. Biophys. Acta* **196,** 53–65.
20. Le Bihan, D., Turner, R., Douek, P. & Patronas, N. (1992) *Am. J. Roentgenol.* **159,** 591–599.
21. Hajnal, J. V., Doran, M., Hall, A. S., Collins, A. G., Oatridge, A., Pennock, J. M., Young, R. & Bydder, G. M. (1991) *J. Comput. Assist. Tomogr.* **15,** 1–18.
22. Moseley, M. E., Cohen, Y., Mintorovitch, J., Chilevitt, L., Shimizu, H., Kucharczyk, J., Wendland, M. F. & Weinstein, P. R. (1990) *Magn. Res. Med.* **14,** 330–446.
23. Knight, R. A., Ordidge, R. J., Helpern, J. A., Chopp, M., Rodolosi, L. C. & Peck, D. (1991) *Stroke* **22,** 802–808.
24. Garcia, J. H. & Anderson, M. L. (1989) *Crit. Rev. Neurobiol.* **4,** 303–324.
25. Schuier, F. J. & Hossman, K. A. (1980) *Stroke* **11,** 593–601.
26. Maxwell, J. C. (1873) *Treatise on Electricity and Magnetism* (Dover, New York).
27. Sen, P. N., Scala, C. & Cohen, M. H. (1981) *Geophysics* **46,** 781–795.